Potential and limitations of resonant tunneling diodes

C. Kidner, I. Mehdi, J. R. East, and G. I. Haddad
Center for High-Frequency Microelectronics and Center for Space Terahertz Technology
Department of Electrical Engineering and Computer Science
The University of Michigan
Ann Arbor, Michigan 48109

Abstract

The existence of negative resistance in double barrier resonant tunneling structures has led to the proposal of various applications for these devices. For useful applications the bias circuit must be free of low frequency oscillations. Stability criteria for resonant tunneling diodes are investigated showing the effect of different modes of low frequency oscillation. The main results of the paper are (1) stable resonant tunneling diode operation is difficult to obtain, (2) the low frequency oscillation introduces a characteristic signature in the measured dc I-V characteristic, (3) the circuit and device conditions required for stable operation greatly reduce the amount of power that can be produced by these devices.

I Introduction

Though the double barrier structure has become a useful prototype mesoscopic device, its usefulness as an electronic device will be determined by functionality rather than by interesting physics. The proposal [1] and later confirmation [2] of the resonant tunneling concept led to the investigation of double barrier structures for various applications. An important potential application is a two terminal negative resistance device, the Resonant Tunneling Diode (RTD), for microwave and millimeter-wave operation [3,4,5,6]. Since the negative resistance of a resonant tunneling device extends from DC to beyond the operating frequency, potential problems exist with low frequency (LF) bias circuit oscillations. A negative resistance device in combination with the bias circuit should be low frequency stable when biased in the negative resistance region for most practical applications. In mixer and detector applications, the LF oscillations can occur near the IF or video frequencies

introducing additional noise. In high frequency oscillator applications LF bias circuit instabilities introduce unwanted upconverted signals that modulate the carrier, resulting in a signal which is not useful for most applications. The paper is organized as follows. The next section contains an analysis of stability conditions for resonant tunneling diodes. The analysis is similar to earlier work on tunnel diodes. Section III contains experimental data to confirm the predictions of the theory. It is shown experimentally that each instability affects the measured I-V curve in a particular fashion. Requiring stability will reduce the power available from resonant tunneling devices. This effect is discussed in section IV.

II Low frequency stability analysis

Assuming the RTD has the same equivalent circuit as a tunnel diode implies that the stability criteria developed for tunnel diodes [7] will also apply in the RTD case. The RTD and the tunnel diode are voltage controlled negative resistance devices. This means that the device will be connected through a bias circuit to a voltage source. In a practical circuit the bias circuit will include the power supply source impedance and various parasitic elements. If the device with its bias circuit is not short circuit stable there will be unwanted oscillations in the bias circuit. A two terminal circuit is short circuit stable if there are no zeroes of the impedance for complex frequencies with positive real parts. In the early 1960's many papers concerning tunnel diode stability were published. While some applications called for short circuit unstable devices [8] the general advice was to only use devices which are short circuit stable [8,9]. In this section we will describe the requirements for stable RTD operation.

Fig. 1(a) shows an equivalent circuit for a RTD including parasitic elements in a waveguide circuit. The circuit between nodes 0 and 1 represents the intrinsic device. $-R_d$ is the negative differential resistance of the device. C_d is the device capacitance, and R_{sd} is the positive parasitic resistance of the device. The circuit between nodes 2 and 1 represents the coupling of the device to the waveguide circuit with L_p representing the inductance of the whisker contact. A resistance R_p within the waveguide cavity can be introduced to improve the device stability. The RF signal

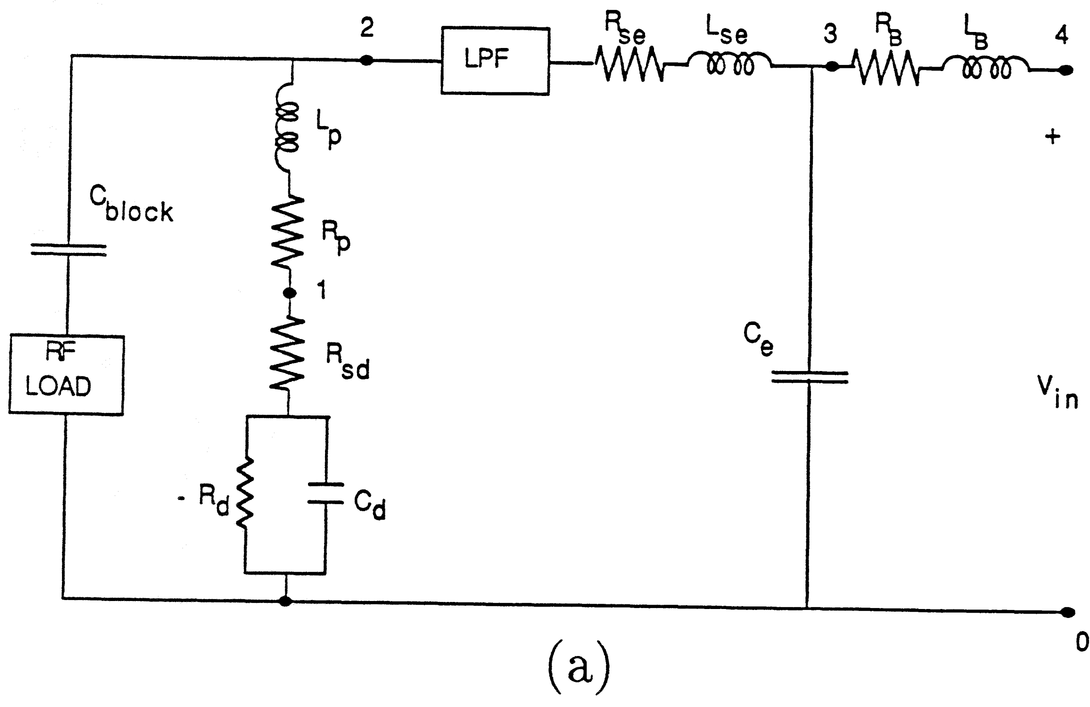

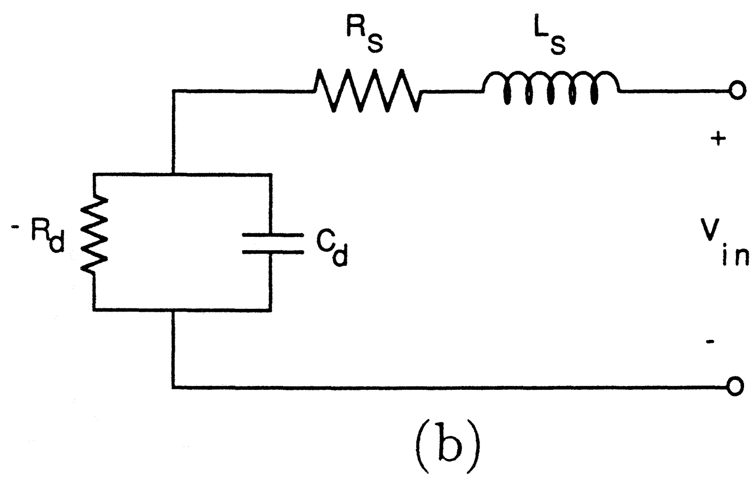

Figure 1: An equivalent circuit for resonant tunneling diodes (a) inside a waveguide circuit, (b) with a simple bias circuit.

is isolated from the bias circuit by a Low Pass Filter (LPF). At low frequencies the LPF can be ignored. The bias signal is isolated from the RF load, modeled here by the blocking capacitor C_{block}. R_{se}, L_{se} and C_e are circuit elements outside of the oscillator cavity. These elements can be used in an attempt to improve the low frequency stability without effecting the RF impedance seen by the device. Finally, R_B and L_B represent the source resistance and inductance of the power supply.

The impedance of the diode coupled to the cavity (across nodes 2 - 0) is

$$Z_{coupled} = R_s + \frac{-G_d}{G_d^2 + \omega^2 C_d^2} + j\omega \left(L_s - \frac{C_d}{G_d^2 + \omega^2 C_d^2} \right), \tag{1}$$

where $G_d = 1/R_d$, $L_s = L_p$ and $R_s = R_p + R_{sd}$. If the magnitude of R_s is less than R_d then the real part of $Z_{coupled}$ is negative at low frequencies and this negative resistance decreases as a function of ω. At the angular frequency ω_r given by

$$\omega_r = \frac{G_d}{C_d} \sqrt{\frac{1}{R_s G_d} - 1}, \tag{2}$$

the real part of the impedance is zero. This frequency corresponds to f_{max}, the cutoff frequency of the diode. Above this frequency the device can no longer supply power to the circuit. At the angular frequency ω_x given by

$$\omega_x = \sqrt{\frac{1}{L_s C_d} - \frac{G_d^2}{C_d^2}}, \tag{3}$$

the imaginary part of Eq. 1 becomes zero. It will be shown that ω_x should be larger than ω_r to prevent spurious oscillations.

For a simple stability analysis the circuit of Fig. 1(a) is approximated by the circuit of Fig. 1(b). This assumes the frequencies of any bias circuit oscillations are low enough that the RF load may be neglected. It also neglects the stabilizing capacitor, C_e. The effect of the stabilizing capacitor will be discussed later. Several of the circuit elements in Fig. 1(a) are in series and thus may be combined to give the elements in Fig. 1(b), $L_s = L_p + L_{se} + L_B$ and $R_s = R_{sd} + R_p + R_{se} + R_B$. The resulting circuit, Fig. 1(b), was studied by Hines [7] for the tunnel diode case.

The circuit in Fig. 1(b) is described by the differential equation

$$L_s C_d \frac{d^2 V}{dt^2} + (R_s C_d - L_s/R_d) \frac{dV}{dt} + V(1 - R_s/R_d) = V_{in}. \tag{4}$$

$V_{in} = 0$ for the short circuit case. The characteristic equation of the above differential equation has four possible solutions but it can be shown that only two solutions lead to a stable circuit [7,10]. The four possible solutions are shown as four different areas in the stability diagram of Fig. 2. The circuit is stable when the solution is exponentially decaying (region III) or exponentially decaying sinusoid (region IV). Combining these gives the stability criteria for the circuit of Fig. 1(b) as

$$\frac{L_s}{C_d R_d^2} < \frac{R_s}{R_d} < 1. \tag{5}$$

Algebraic manipulation shows that the first inequality of Eq. 5 is equivalent to

$$\omega_r < \omega_x$$

as a stability criteria, with the frequencies defined in equations 2 and 3.

To obtain stability the ratio R_s/R_d should be just less than one so that both inequalities of Eq. 5 can be satisfied. Not all of R_s has to be part of the rf circuit. R_s consists of four separate positive resistances. R_{sd} is the positive resistance associated with the device and is largely dependent on device design and fabrication. R_p is also part of the rf circuit and may be used to stabilize the RTD. If C_e is not included, R_B is indistinguishable from R_s. The stabilizing load may be inside (R_p) or outside (R_{se}) the rf circuit. Circuit stabilization is often simpler when R_p is sufficient to stabilize the circuit [11]. However, this will degrade the power generation capability of the diode since there will be more positive resistance associated with the device. If the stabilizing load is in the rf portion of the circuit then nearly all the rf power is lost to the stabilizing load. So if possible the bias line stabilizing load should be isolated from the rf circuit.

Typically, for RTDs with peak currents in the mA range R_d is tens of ohms or less and C_d is tens of pF. This constrains L_s to nH's or even tenths of a nH. Since a whisker contact introduces an inductance of this order many RTDs are difficult to stabilize when used with whisker contacts. It is interesting to study the effect of the series inductance L_s. For a given device and circuit, the external inductance in the bias circuit can be varied to sample different portions of the stability plot in Fig. 2. Experimental bias circuit oscillations of a resonant tunneling diode mounted in a low inductance whisker contact cavity with a variable external lead inductance are shown in Fig. 3.

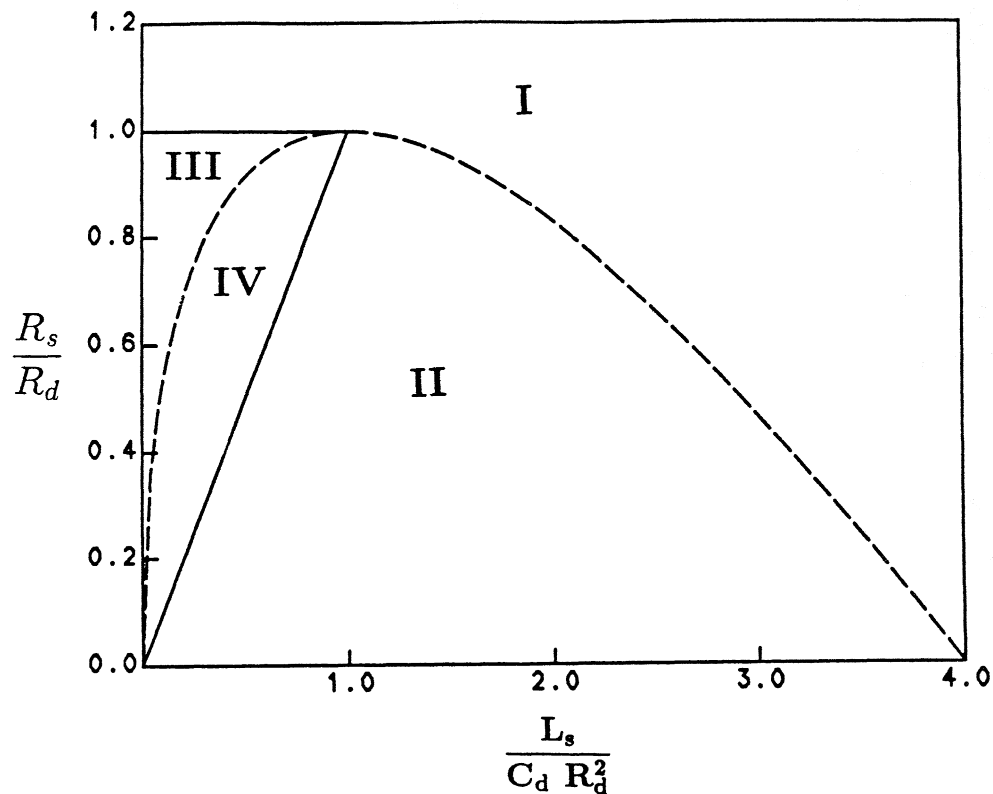

Figure 2: The stability diagram for resonant tunneling diodes based on circuit and device parameters. Regions III and IV correspond to a short circuit stable circuit.

The device is a resonant tunneling diode with AlAs barriers that are 30 Å, thick, an $In_{0.10}Ga_{0.90}As$ deep well that is 70 Å wide, and spacer layers on each side that are 30Å wide. The contact regions are doped to $2 \times 10^{18} cm^{-3}$. Standard photolithiography techniques are used to fabricate diodes of various sizes. The measurements are done on 50 μm by 50 μm diodes.

The circuit is in region I of Fig. 2 for very large L_s. Devices biased in region I should have a growing exponential waveform. In reality,the growth is limited by the extent of the negative resistance region. The result is the well known relaxation oscillation. Similar conditions occur in a tunnel diode [9]. The voltage across the bias terminals of the experimental device is shown in Fig. 3(a). For smaller values of L_s ,the operating point moves to the left on the stability curve in Fig. 2 into region II. The stability diagram predicts growing sinusoidal oscillations, which are also limited by the extent of the negative resistance region. This results in a nearly sinusoidal steady state oscillation and a measured case is shown in Fig. 3(b). In the growing sinusoid region, decreasing L_s causes the frequency of oscillation to increase. This is shown by differentiating the frequency of

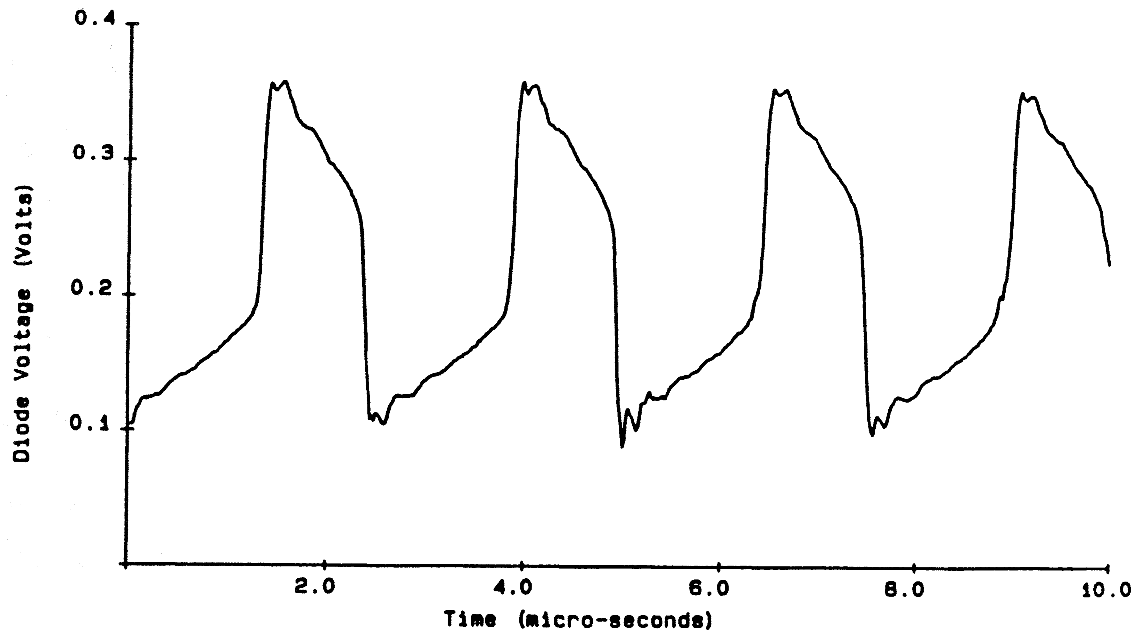

(a)

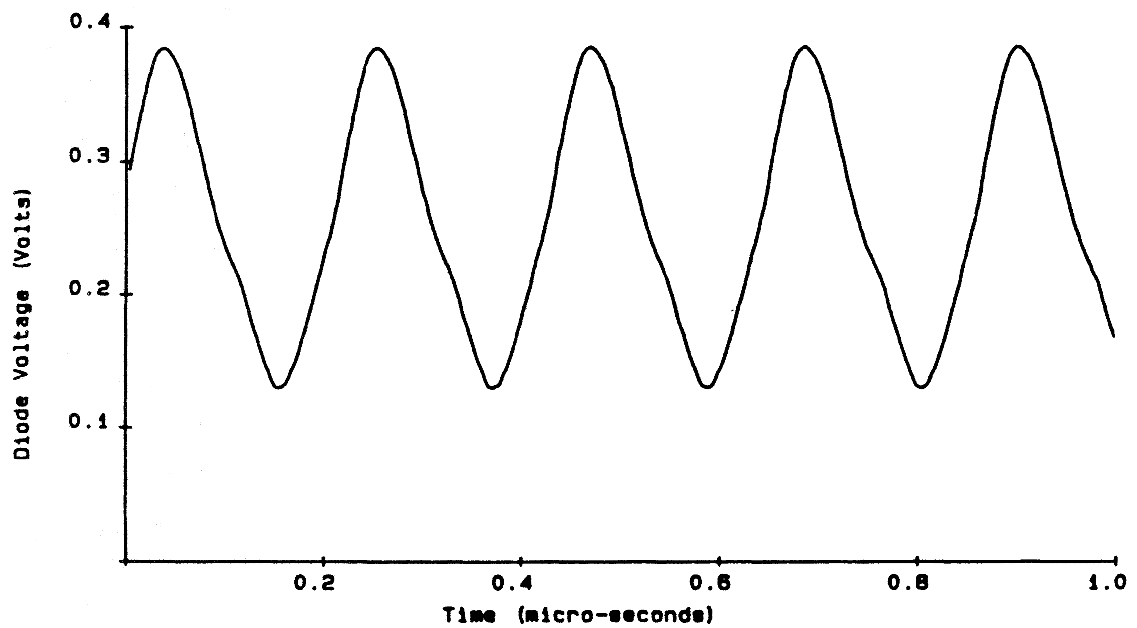

(b)

Figure 3: Low frequency oscillation of the RTD as measured by an oscilloscope (a) in the growing exponential region(area I) of the stability diagram. A large RF choke was placed in the bias lines to produce this oscillation. (b) in the growing sinusoidal region (Area II) of the stability diagram. The inductance is from approximately 2 meters of lead wire.

oscillation with respect to the series inductance to obtain

$$\frac{d\left(\omega^2\right)}{dL_s} = \frac{1}{4C_d^2L_s^3}\left(2L_sC_d\left(\frac{R_s}{R_d} - 2\right) + 2R_s^2C_d^2.\right) \tag{6}$$

For large L_s this is negative since $R_s/R_d < 1$. The extrema is then found by setting the above equation equal to zero and solving for L_s. An extrema occurs when

$$L_s = \frac{R_s^2C_d}{2 - \frac{R_s}{R_d}} < R_s^2C_d < R_sR_dC_d.$$

Since the denominator of the derivative is linearly decreasing with L_s this is a maximum. This means that the maximum frequency occurs for values of L_s smaller than the value required for stability. Now, if one calculates the oscillation frequency when L_s is just small enough to give stability one obtains

$$\omega = \frac{1}{R_dC_d}\sqrt{\frac{R_d}{R_s} - 1} = \omega_r. \tag{7}$$

This gives physical meaning to the stability conditions. For a given device R_d and C_d are fixed. Assuming R_s is less than R_d the circuit L_s controls the stability. The idea is to decrease L_s which in turn increases the oscillation frequency until the oscillation frequency is above the resistive cutoff frequency of the device.

A common method for stabilizing a tunnel diode or RTD is to place a capacitor in shunt across the terminals of the device [7,12,13]. From the preceeding analysis it is seen that instability would be overcome if the DC source could be inserted physically near the RTD, minimizing the inductance. Since a large shunt capacitor will appear to the bias circuit oscillations as a DC voltage source the capacitance, C_e shown in Fig. 1(a) effectively accomplishes this. Fig. 4(a) is the same circuit with series elements combined: $L_s = L_p + L_{se}$ and $R_s = R_{sd} + R_p + R_{se}$. To study the effect of C_e the circuit is broken into separate high- and low-frequency equivalents, both of the form of Fig. 1(b). For high frequencies C_e is a short circuit so the combination of L_s, R_s, R_d and C_d in Fig. 4(a) must satisfy the stability criteria, Eq. 5. For the low frequency circuit the element values in Fig. 1(b) become $L_s = L_B$, $R_s = R_B$, $R_d = R_d - R_{sd} - R_p - R_{se}$ and $C_d = C_e$. This low frequency equivalent R_d is different than that given by Hines [7]. The value given here is chosen to give the correct impedance at DC. Plotting the impedance locus vs. frequency for various element values

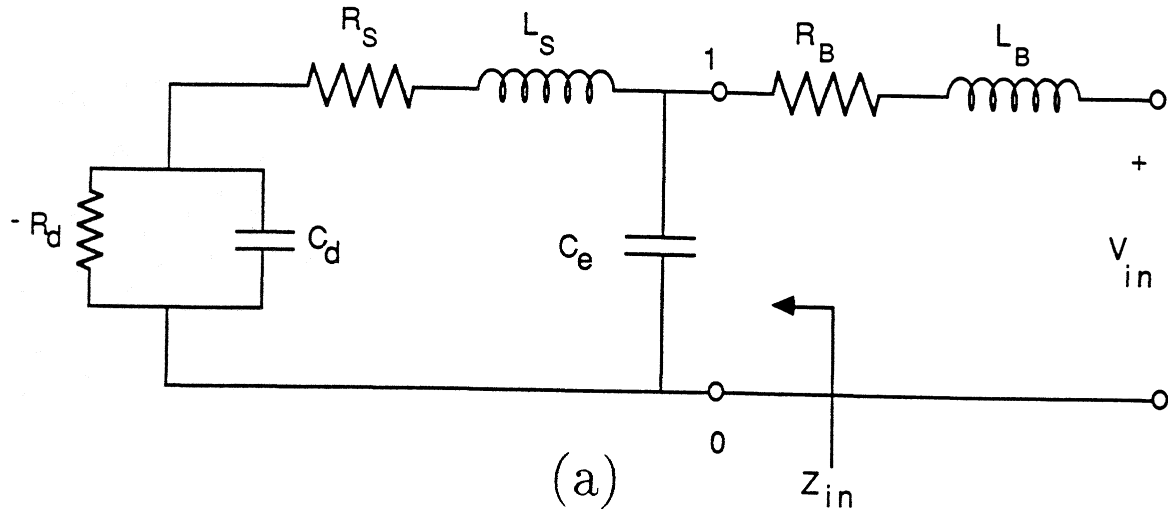

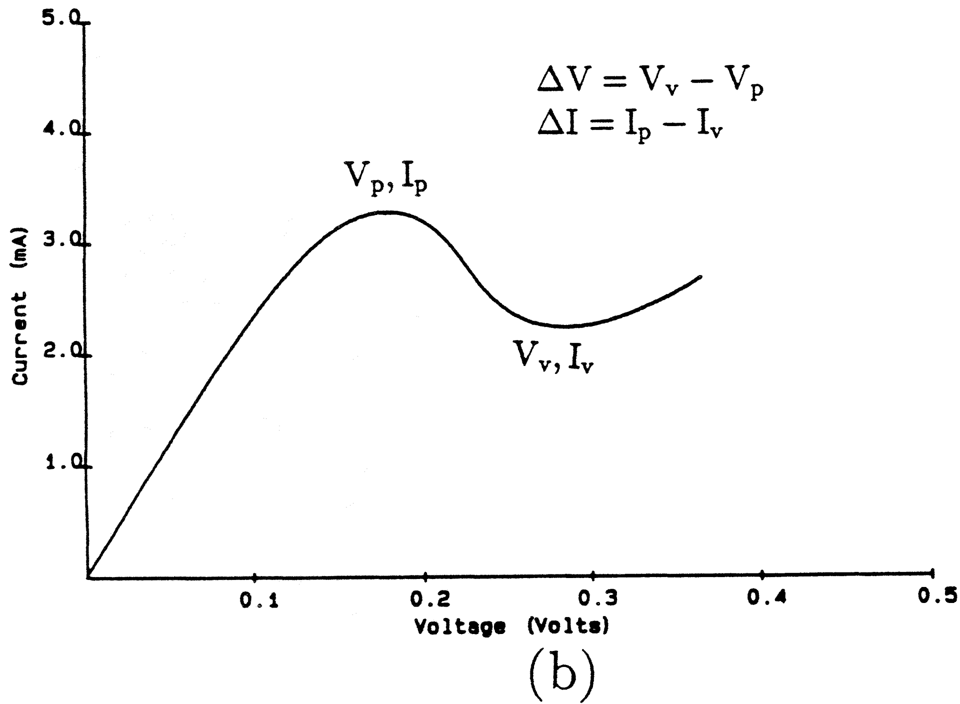

Figure 4: (a) Use of an external capacitance for stabilization, (b)the "true" stable DC I-V curve for the device under consideration as measured on the HP 4145 semiconductor parameter analyzer. Stabilization was attained using $R_s = 33\Omega$ and $C_e = 0.1\mu F$.

indicates that this approximation is very good when the high frequency circuit is stable. Then a sufficient condition for the circuit in Fig. 4(a) to be stable is

$$\frac{L_s}{R_d^2 C_d} < \frac{R_s}{R_d} < 1 \quad AND \quad \frac{L_B}{(R_d - R_S)^2 C_e} < \frac{R_B}{(R_d - R_s)} < 1 \tag{8}$$

The circuit of Fig. 4(a) was used to stabilize the diode discussed earlier with $R_s = 33\Omega$ and $C_e = 0.1\mu F$. The diode was considered stable when no oscillations could be detected using an oscilloscope across the bias leads. Care was taken to ensure that the frequency of the oscillations, usually hundreds of MHz, was not greater than the bandwidth of the oscilloscope. The stable I-V curve of Fig. 4(b) is felt to represent the "true" I-V curve.

The condition of eq. 8 is not necessary. However, Nyquist analysis of the full circuit for different element values indicate that while it is theoretically possible to obtain a stable circuit when the high frequency circuit is unstable, stability requires precise element values and could not be attained in practice. If the simple stability conditions, Eq. 5, are not met by the circuit shunted by the external capacitance, stable operation of the circuit in Fig. 4(a) is virtually unobtainable.

III Low frequency I-V characteristics of unstable devices

The effect of various intrinsic and extrinsic circuit elements on the measured DC I-V characteristics of unstable devices will be discussed in this section. It is shown that from the shape of the I-V characteristic one can tell what kind of instability is present in the circuit. This analysis is not only useful for its own sake but it is necessary since the instability can have severe consequences on the device applications. Some preliminary work on this subject has been described by Young et. al. [3] and Liu [12]. The circuit of Fig. 1(b) will be used for the discussion of DC I-V curves in this section. The same diode as in section II is used to experimentally demonstrate the conclusions. Bias oscillations distort the measured I-V characteristic away from the "ideal" curve of Fig. 4. Three classes of distortions are commonly observed: switching; bistability; and bias circuit oscillations. Sometimes more complex distortions such as double plateau structures are observed which have not been investigated.

An I-V curve displaying switching is shown in Fig. 5. This type of distortion is discontinuous in

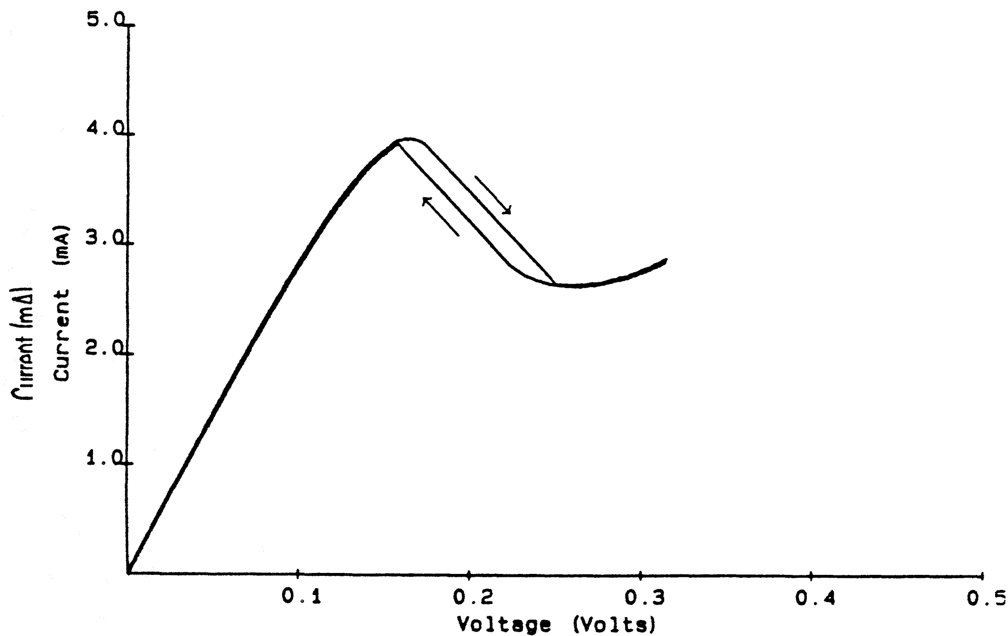

Figure 5: The measured diode I-V curve with an "external" resistance, $R_s \approx 55\Omega$. The "switching" of the diode is obvious.

both current and voltage. This behavior is due to a large series resistance between the voltage source and the point at which the voltage is measured. In the inset of Fig. 6 this corresponds to measuring I vs. V_D with $R_s > |R_d|$ in the NDR region. The resulting I-V curve is apparent from load line analysis on the stable I-V characteristic shown in Fig. 4. As V_{in} is increased from zero to $V_p + R_s I_p$ the measured I-V curve faithfully reproduces the true I-V curve. Since no negative resistance is present the circuit is stable and there is no switching in the region $V_v + R_s I_v < V_{in} < V_p + R_s I_p$ where the load line intersects the I-V curve at three different points. When V_{in} is increased beyond $V_p + R_s I_p$ the only stable point is on the right positive resistance portion of the I-V curve, forcing switching behavior. When V_{in} is swept from $V_{in} > V_p + R_s I_p$ the same argument holds. Hysterisis occurs because the positive going switch point, $V_{in} = V_p + R_s I_p$ is less than the negative going switch point, $V_{in} = V_v + R_s I_v$. Since $R_s > |R_d|$ it follows from the stability diagram, Fig. 2, that the voltage is varying exponentially with time.

An I-V curve showing bistability in the present device due to an internal resistance is shown in Fig. 6. For purposes of demonstration a large series resistance was added which was treated as

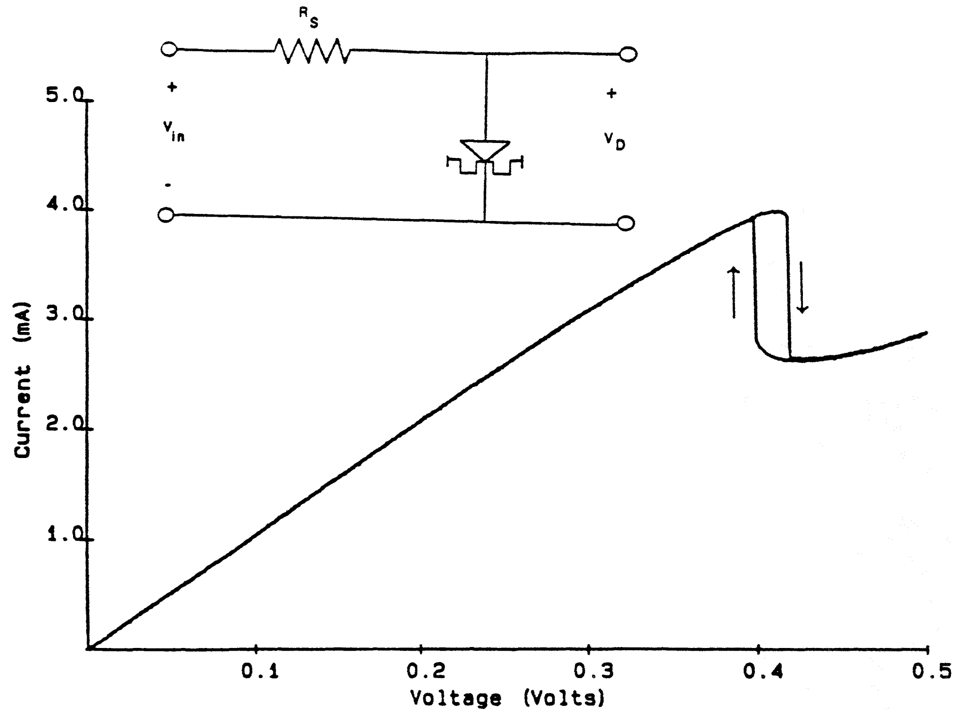

Figure 6: Diode measured I-V curve showing the bistable nature of the device due to an "intrinsic" series resistance $R_s \approx 55\Omega$).

"internal." In practice the internal series resistance is usually the positive resistance of the device independent of the measuring apparatus. This resistance includes contact resistance and epilayer resistance. The distinctive feature of this distortion is that only the current is discontinuous. This behavior is due to a voltage drop between the point at which the voltage is measured and the NDR device. In the inset of Fig. 6 this corresponds to measuring I vs. V_{in} with $R_s > |R_d|$. Load line analysis follows that presented for the switching case , with similar results. An important difference between the two distortions is that an internal resistance always distorts the I-V curve while an external resistor only distorts the curve if $R_s > |R_d|$.

An I-V curve displaying a plateau structure is shown in Fig. 7. It is a simple matter to show by numerical methods that such a structure is to be expected when bias circuit oscillations are present [2]. The measured current is simply the time average of the current waveform. It does not involve a detection process, so the term "self detection" is a misnomer. These oscillations occur when

$$\frac{R_s}{R_d} < \frac{L_s}{R_d^2\, C_d} < 1 \qquad (9)$$

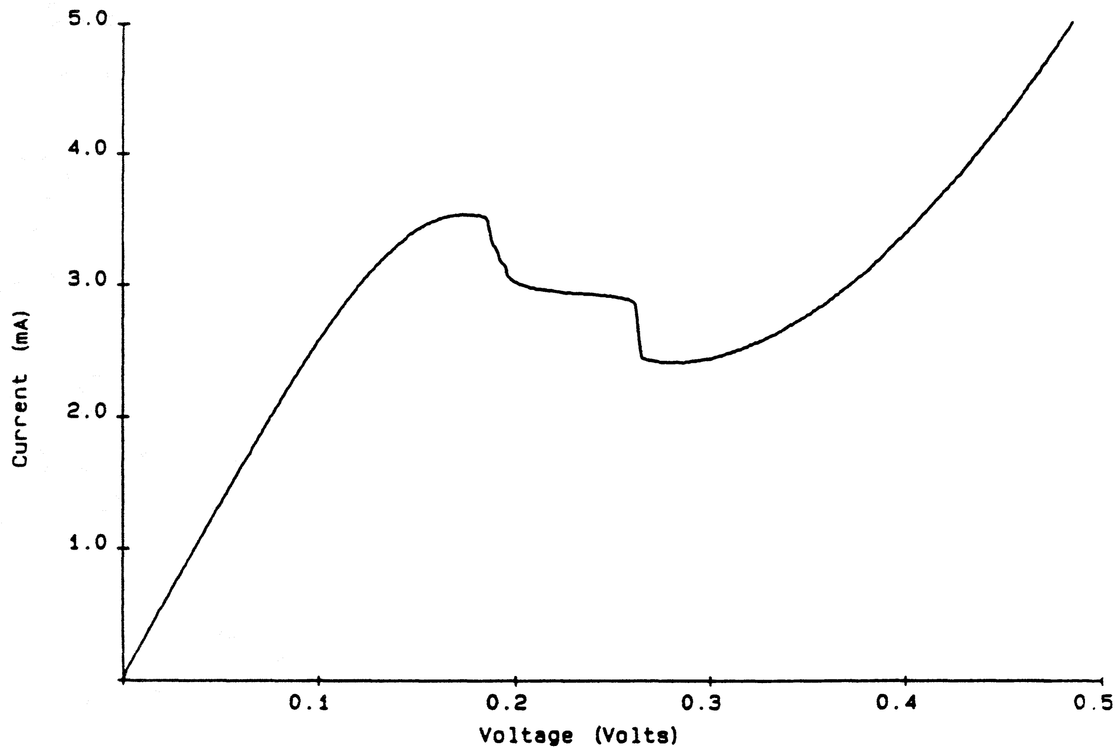

Figure 7: Measured I-V curve showing a plateau structure because of bias circuit oscillations.

For the device tested the DC I-V curve was insensitive to whether the oscillation was sinusoidal or relaxation, Fig. 3(a) or 3(b).

IV Effect of device stability on power generation

The purpose of this section is to show the effect of the stability requirements on the power generation capability of RTDs. Assuming the designer has control of R_s, ($R_s/R_d \approx 1$) the inequality for a stable negative resistance device can be written as

$$C_D > A_D \times G_D^2 \times L_s \tag{10}$$

where now A_D is the device area and the capacitance, C_D , and conductance, G_D, are now per unit area. Thus to obtain stable devices one must decrease the device area, the conductance and the series inductance and increase the device capacitance. Let us now examine each element in more detail regarding stability and high frequency power generation.

Both the negative resistance and the series resistance of the device are frequency dependent. It has been shown from theoretically calculated characteristics that for a particular device the negative

conductance remains constant up to about 200 GHz but then starts to decrease and in the terahertz range becomes about half of the DC value [14]. This is certainly device dependent and for some devices the roll off will be much faster. Similarly the series resistance of the device, assuming contact resistance and epilayer resistance to be constant, increases as a function of frequency mainly due to the behaviour of the skin depth [15]. This behaviour was not considered in the stability analysis, where the circuit values are considered to be constant. Physically it is clear that this will not produce bias circuit oscillations since the effect is to lower the resistive cutoff frequency. Such roll off will, however, further limit the power generating capabilities of RTDs at very high frequencies.

Decreasing the device area is consistent with requirements for high frequency devices. By reducing the device area the device capacitance is reduced which is beneficial in coupling these low impedance devices to the RF load. The limit on device area is imposed by the relevant fabrication technology and packaging restraints. One micron diameter Schottky diodes have been fabricated but diameters much smaller than this might be hard to obtain. Extremely small diodes will be very difficult to contact. Even if the device can be contacted, it may be too small to produce any useable power.

The physical origin of L_s is the inductance due to the lead that connects the device to the measuring apparatus or the device package. For practical applications the devices can be contacted either with bond wires or through whisker contacts. At low frequencies the devices are usually bonded in microwave packages and the associated inductance is at least 1 nH. For high frequency operation whiskers are used and the corresponding inductance depends on the diameter and length of the probe. An approximate inductance value for this configuration is about 0.2 nH [16]. The goal of reducing series inductance for stability is consistent with the requirements for high frequency operation. However, it should be realized that with conventional contacting techniques inductance lower than 0.2 nH can not be easily obtained.

The origin of the device capacitance is the charge distribution in the device. Since the double barrier structure is an undoped region sandwiched between two moderately or heavily doped regions, the device capacitance can be approximated by a parallel plate capacitance model. A

more accurate value of the device capacitance may be found by using a self consistent quantum mechanical simulation to calculate the width of the depletion region. The goal of increasing device capacitance for stability is in direct conflict with performance criteria for high frequency devices [17].

The device negative conductance is given by $\Delta I/\Delta V$, assuming that the negative resistance region is linear. For stability the conductance should be decreased as much as possible implying that ΔI should be reduced and ΔV should be increased.

To calculate the power output from resonant tunneling devices the device area must be selected. One method for calculating the area is to assume that the device is matched to a circuit with resistance of R_L ohms. In that case, the device area can be written as:

$$A_D = \frac{1}{(R_L + R_s)} \times \frac{G_D}{G_D^2 + (\omega C_D)^2} \tag{11}$$

where R_s is the device series resistance, G_D is the conductance per unit area of the device. C_D is the capacitance per unit area of the device under consideration. From the above equation it is seen that the device area becomes larger as $(R_L + R_s)$ is reduced. Since the power scales with device area, it is desirable to reduce the series and circuit resistances as much as possible. In the analysis presented here, it is assumed that the minimum achievable circuit resistance is 1-Ω and the series resistance of the device is negligible. This is an approximation and will be difficult to realize at very high frequencies. However, if a larger load or series resistance is present, then the output power will scale inversely with the load resistance. With the assumption that R_L is equal to 1-Ω and R_s is negligible,

$$A_D = \frac{G_D}{G_D^2 + (\omega C_D)^2}. \tag{12}$$

The rf power achievable from the device for the given area is then calculated as

$$P_{RF} = \frac{1}{2}\frac{{V_{rf}}^2}{1 + \left(\frac{\omega C_D}{G_D}\right)^2}, \tag{13}$$

where V_{rf} is the peak rf voltage. The magnitude of V_{rf} is selected to be half of ΔV and assuming

$G_D = \Delta I/\Delta V$ then the expected power at very high frequencies can be written as [5,17]

$$P_{RF} = \frac{1}{8\omega^2}(\frac{\Delta J}{C_D})^2, \tag{14}$$

where ΔJ is the difference between the peak current and the valley current. Driven by this rule the effort has been to increase the current density and decrease the device capacitance while maintaining a reasonable peak to valley current ratio. However, no consideration was given to stability in that analysis. If stability is considered then the analysis is no longer strictly valid except for an ideal situation where the inductance L_s is negligible. The obvious change is that there is a lower bound on the capacitance of the device. This bound is given by $C_d > L_s/R_d^2$. Decreasing the capacitance beyond this point will make the device unstable.

Moreover, the peak current density is no longer the dominant parameter in the figure of merit. In fact, when the device is limited by stability, the performance becomes inversely related to the ratio of peak current to device capacitance. Rearranging Eq. 10 gives

$$A_D < \frac{C_D}{L_s G_D^2}. \tag{15}$$

So then the stability limited power becomes

$$P_{RF} \leq \frac{1}{8}\Delta V \Delta J \frac{C_D}{L_s G_D^2} \tag{16}$$

which, assuming a linear negative resistance region reduces to

$$P_{RF} \leq \frac{1}{8L_s}(\Delta V)^3 \frac{C_D}{\Delta J}. \tag{17}$$

This clearly demonstrates that ΔV cannot be ignored when designing devices for high frequency power generation.

Thus there are two rf circuit parameters which can limit the power from a device, the minimum achievable load resistance and the minimum achievable lead inductance. The minimum load resistance limits the diode area which can be made to oscillate at the desired frequency. The minimum inductance limits the diode area which will not oscillate with the bias circuit. The power from a device will not be limited by stability concerns if P_{RF} in Eq. 17 is greater than P_{RF} in Eq. 14.

Combining these equations reduces to

$$\Delta V > \frac{\Delta J}{C_D}\left(\frac{L_s}{\omega^2 R_L}\right)^{1/3}. \tag{18}$$

Or, in terms of the circuit parameters

$$\frac{\omega L_s}{R_L} < \left(\frac{\Delta V \omega C_D}{\Delta J}\right)^3. \tag{19}$$

From the above discussion and analysis it can be seen that the criteria for stability do not always coincide with the criteria for high frequency operation.

The effect of requiring stability is demonstrated using a typical device. A self consistent quantum mechanical simulation [18] was used to generate the I-V characteristic. For this particular device the barrier height was selected to be 0.24 eV, the barrier and well width was 23.3 and 43.5 Å respectively. The doping outside the barriers was 1×10^{17} and spacer layers of 50 Å were used. Also a 100 Å drift layer was used on the anode side. These parameters correspond to a GaAs/AlGaAs device which can be fabricated. From the computer simulation this device has a peak current density of $8.6 \times 10^4 \mathrm{A/cm^2}$, peak-to-valley current ratio of 4, a $\Delta \mathrm{V} = 0.24\mathrm{V}$, and a depletion region width of 491 Å.

Fig. 8 shows the results of the rf power calculation using Eq. 14 as well as the device area matched for 1 ohm circuit matching (upper curves). This analysis does not take into consideration the series resistance of the device which could further degrade the device performance. Now, for comparison we invoke the stability criteria. We assume that this device can be contacted so that the series inductance is 1 nH. Using this one finds that the device is unstable when matched to a 1 ohm load (the device area is too large to be stabilized). Using Eq. 15 we find that the device will be stable if the area is $3 \times 10^{-9} cm^2$ or less. Thus stabilizing the device places severe constraints on the device size. The maximum area corresponds to a circular mesa of 0.4 μm diameter which would be extremely difficult to contact. If one was somehow able to fabricate and contact this device and assuming that the series inductance is still 1 nH then the available power, from Eq. 17 is shown in Fig. 8 (lower curves) for matching to a non constant load resistor. Note the decrease in output power. The required area and output power assuming that a [illegible] inductance of 0.2 nH was obtainable is also shown in Fig. 8.

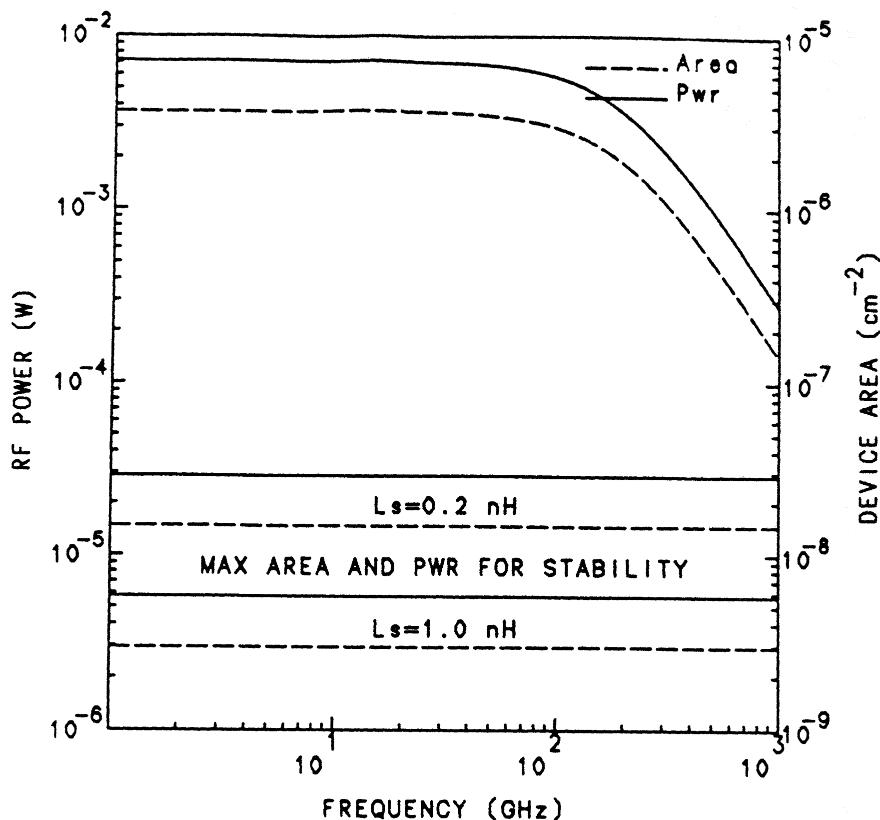

Figure 8: Expected power and area necessary for matching into a 1 ohm resistance (top curves). The lower curves indicate the maximum area and power attainable from the same device if the device was made stable (assuming two different L_s values).

It is apparent from the above results that if one fulfills the requirement for stability the power generation capability of the device is significantly compromised even if it is possible to obtain the required small areas. Since the device conductance and capacitance are fixed the only other circuit element that can be varied is the series inductance. In Table 1 the maximum diode diameter, corresponding power at 1000 GHz and the necessary load resistance are calculated for different values of the series inductance. In all the calculations R_s has been assumed to be negligible when compared to R_L. This approximation is not valid when R_s becomes comparable to R_L. For $R_s = R_L$ the useful power deleivered to R_L will be reduced by half of that shown in the Table. It is also worth noting that decreasing the diode diameter will increase R_s in an actual device.

V Conclusion

The stability criteria for resonant tunneling diodes have been derived. Based on the criteria it is shown that stable operation of resonant tunneling diodes is hard to obtain. The importance of

L_s	At 1 THz		
	d_{max}	P_{max}	R_L
nH	μm	μW	Ω
25	0.06	0.23	1191
10	0.10	0.58	476
5	0.14	1.15	238
2	0.22	2.88	95.4
1	0.31	5.75	47.7
0.5	0.43	11.5	23.8
0.2	0.69	28.8	9.54
0.1	0.97	57.5	4.77

Table 1: Maximum diode diameter(in microns), maximum power generation (in microwatts) and corresponding load resistance (in ohms), at 1 THz for various lead inductances when the device is stable.

circuit inductance cannot be over emphasized. In order to stably bias an RTD the lead inductance must be minimized. The diodes can be made stable by using a shunt capacitor but this is only possible if the circuit inductance is very small. It was shown that each instability produces a signature I-V characteristic. The expected I-V curves were experimentally produced using a diode which could be stabilized. Finally, the effect of stability criteria on the potential and capability of RTDs for high frequency power generation has been studied. Requiring stability for devices severly limits the diode area. It is shown that the device parameter ΔV will have a very strong influence on the performance of high frequency RTDs if the lead inductance is not negligible.

Acknowledgments

The authors wish to thank Dr. Richard Mains for many helpful discussions. This work was supported by the NASA Center for Space Terahertz Technology under contract no. NAGW-1334 and the US Army Research Office under the URI program, contract no. DAAL03-87-K-0007.

References

[1] R. Tsu and L. Esaki. *Appl. Phys. Lett.*, 22(11):562–564, June 1973.

[2] L. L. Chang, L. Esaki, and R. Tsu. *Appl. Phys. Lett.*, 24:592–595, 15 June 1974.

[3] T. C. L. G. Sollner, W. D. Goodhue, C. D. Parker P. E. Tannenwald, and D. D. Peck. *Appl. Phys. Lett.*, 43(6):588–590, September 1983.

[4] W. R. Frensley. *Appl. Phys. Lett.*, 51:448–450, 10 August 1987.

[5] R. K. Mains, I. Mehdi, and G. I. Haddad. *Intl. Journal of Infrared and Millimeter Waves*, 10(6):595–620, June 1989.

[6] V. P. Kesan, A. Mortazawi, D. P. Niekirk, and T. Itoh. *IEEE-MTT-S Digest*, 1(L-39):487–490, June 1989.

[7] M. E. Hines. *Bell Syst. Tech. J.*, 39:477–513, May 1960.

[8] H. A. Watson. *Microwave semiconductor devices and their circuit applications.* McGraw-Hill Inc., 1969.

[9] W. F. Chow. *Principles of Tunnel Diode Circuits.* John Wiley and Sons, 1964.

[10] C. Kidner, I. Mehdi, J. East, and G. Haddad. *Submitted to Solid-State Electronics*, Copies available upon request.

[11] J. M. Owens, D. J. Halchin, K. L. Lear, W. S. Lee, and J. S. Harris Jr. *MTT-Digest*, 1:471–474, June 1989.

[12] H. C. Liu. *Appl. Phys. Lett.*, 53(6):485–486, August 1988.

[13] J. F. Young, B. M. Wood, H. C. Liu, M. Buchanan, D. Landheer, A. J. SpringThorpe, and P. Mandeville. *Appl. Phys. Lett.*, 52(17):1398–1400, April 1988.

[14] R. K. Mains and G. I. Haddad. *J. Appl. Phys.*, 64(7):3564–3569, October 1988.

[15] E. R. Brown, W. D. Goodhue, and T.C.L.G Sollner. *J. Appl. Phys.*, 64(3):1519–1529, August 1988.

[16] M. A. Frerking. Personal communication.

[17] I. Mehdi, G. I. Haddad, and R. K. Mains. *Optical and Microwave Tech. Lett.*, 2(5):172–175, May 1989.

[18] R. K. Mains, J. P. Sun, and G. I. Haddad. *Appl. Phys. Lett.*, 55(4):371–373, July 1989.